Ultrafine Particles of Iron(III) Oxides by View of AFM – Novel Route for Study of Polymorphism in Nano-world

Milan Vujtek, Radek Zboril, Roman Kubinek and **Miroslav Mashlan**

Departments of Experimental Physics, Inorganic, and Physical Chemistry, Palacky University, Svobody 26, Olomouc 771 46, Czech Republic.

Abstract. *The use of atomic force microscopy for the characterization of Fe_2O_3 nanopowders is discussed and demonstrated with several experimental examples related to the new exhibitions of polymorphism in the nano-world. Due to the rare literature data concerning the application of AFM in the analysis of iron oxide particles, our experimental experience, advantages and drawbacks of this microscopic technique including the comparison with the conventionally used TEM are described. The influence of sample preparation, possible artifacts and image deformations on interpretation of AFM data is emphasized.*

1 Introduction

From the viewpoint of the basic research, iron(III) oxide is a convenient compound for the general study of the polymorphism and the magnetic and structural phase transitions of nanoparticles. The existence of amorphous Fe_2O_3 and four polymorphs (alpha, beta, gamma, epsilon) has been still established [1]. The most frequent polymorphs, the hexagonal corundum structure "alpha" and cubic spinel structure "gamma", have been found in nature as hematite and maghemite minerals. The other polymorphs, the cubic bixbyite structure "beta" and orthorhombic structure "epsilon", as well as nanoparticles of all forms, have been synthesized and extensively investigated in recent years [1-7].

From the viewpoint of the applied research, iron (III) oxide in all its forms is one of the most commonly used metal oxides with various applications in many environmental and industrial fields. Iron oxides are components of several ores used for the production of iron and steel, geologically and archeologically important earth-samples, minerals as well as extraterrestrial materials. Due to their hardness, catalytic activity, surface resistivity and the other exceptional (magnetic, optical, electronic) properties, they are used as abrasives, polishing agents, catalysts, gas sensors, pigments, photoanodes for photoelectrochemical cells or contrast agents in magnetic resonance imaging. They also play an important role in the production of ferrites and in the magnetic prospecting of archeological areas [1,2].

Small iron oxide particles (1-100 nm) exhibit unique features that strongly differ from those of well-crystallized particles. These nanoparticles are of fundamental importance in many of the above mentioned industrial applications, including the development of new electronic and optical devices, information storage, magnetocaloric refrigeration, color imaging, bioproceesing, ferrofluid technology or manufacture of magnetic recording media. The advantage of using Fe_2O_3 nanoparticles relies on their chemical stability, in contrast to the commonly used ultrasmall particles of pure metals [1,2].

On account of attractive scientific and industrial applications of Fe_2O_3 nanoparticles, the novel methods for their synthesis and the new approaches in their characterization have been registered in recent years. Iron(III) oxide nanoparticles with various structures, sizes and morphologies have been attained by oxygen-hydrogen flame pyrolysis, laser pyrolysis, electrochemical synthesis, sol-gel method, vaporization-condensation process in a solar furnace, micro-emulsion technique, diode sputter deposition, thermal decomposition of an aerosol upon a heated substrate, or by thermally induced solid-state reactions of suitable ferrogenous precursors [1].

The conventional analysis of the structural, magnetic and electronic properties of Fe_2O_3 nanoparticles includes the using some of methods as XRD, EPR, ^{57}Fe Mössbauer spectroscopy, SQUID magnetization measurements, magnetic susceptibility measurements, electron energy loss (EEL) spectra, and X-ray absorption spectroscopy (XAS). Both for the study of mechanism of polymorphic changes and for the particular industrial applications of iron oxide nanoparticles, the distinguishing of individual polymorphs and the determination of particle size and morphology have the primary importance resulting in the

extensive use of microscopic techniques in this field. Moreover, the low particle size and the strong tendency of powdered nanoparticles to agglomeration restrict the use and the correct interpretation of some indirect measurements (XRD, DLS, BET measurement of the surface area).

Although the position of TEM (or HRTEM) is dominant at the analysis of Fe_2O_3 systems [7-10], the role of AFM increases step by step. It is mainly due to the three-dimensional images allowing to examine the real particle morphology including the vertical dimension. In the case of an analysis of phase (polymorphic) mixtures, the 3D images give the chance to distinguish the structurally nonequivalent particles on the basis of their size and morphological characteristics (the ratio of lateral and vertical dimensions). The possibility of the determination of some surface characteristics (mean surface roughness, surface fractal dimension) is important from the viewpoint of considering the surface geometry and the degree of the disorder of the surface structure of iron oxides. In the case of Fe_2O_3 nanoparticles, the above-mentioned advantages are limited by the lower lateral resolution due to the tip convolution resulting in the difficult analysis of ultrasmall (<10 nm) particles. On the other hand, different methods and algorithms have been proposed to minimize and/or to determine the influence of a tip convolution [11-13].

In the last years, AFM has been successfully used for the characterization of iron oxides formed in citrate solutions [14], prepared by laser ablation [15], or synthesized as a ferrofluid sample [16]. In this paper, the experimental results, general experience, advantages and drawbacks of AFM in the analysis of Fe_2O_3 particles prepared by thermally induced solid-state reactions of gas liberating Fe materials are presented and documented with several examples.

2 AFM Analysis of Fe_2O_3 Particles – Instrumentation, Sample Processing

AFM measurements of Fe_2O_3 powders were performed using the AFM Explorer microscope (Thermo-Microscopes, USA) in air and at room temperature, in a non-contact mode with Si tips of the 1650-00 type with resonant frequencies ranging from 180 to 240 kHz and with the tip radius less than 10 nm. The microscope was placed on a pneumatic antivibration desk, under a damping cover. The processing was conducted using the SPMLab software, the measurements were realized in the ranges from 2000×2000 nm to 100×100 nm with the resolution of 300×300 pixels.

Iron oxide samples for AFM analyses are necessary to be spread on a suitable surface since they are of a powder character. Synthetically prepared mica (Structure Probe, Grade V-4, USA) has been chosen as the ground. Its topmost layers are ripped off straight before spreading the sample in order to achieve an atomically smooth and clean surface. The iron oxide powder is dispersed in water by using of ultrasonification at 140 W for 3 minutes. Depending on the type of sample, a small addition of sodium hexametaphosphate solution can be applied to inhibit the agglomeration tendencies of ultrafine particles. 20 μl of liquid containing the dispersed nanoparticles are taken using a micropipette immediately after ultrasonification. The dispersed Fe_2O_3 particles are spread on the preheated mica and put into a drying oven to evaporate water.

The drying time and temperature greatly influence the resulting quality and applicability of the sample for measurement. Too long drying time and/or too high temperature result in a significant decrease of the stability of AFM measurement due to the bad fixation of Fe_2O_3 particles on the mica surface. In the case of samples dried at the found optimal conditions (50 °C, 10-15 min.), this fixation is improved since the particles hold in a very thin layer of water (∼1 nm) adsorbed on the mica surface. On the other hand, too short a drying time is manifested by large clustering of particles to one another and/or by the existence of the water joints among particles that often create chains and netted structures (Fig. 1A). If the sample is prepared by drying at higher temperatures (> 80 °C) for a short time (< 5 min.), an unusual distribution of the particles on the mica surface can be observed. Thus 2D clusters, which are very similar in a near environment, may emerge (Fig. 1B). Traces of outlasting water can be found among the individual particles of the cluster. No particles are observed in the near surrounding of these clusters.

The manner of sampling from the test tube (the time after shaking, the sampling depth) is another important factor that can have a considerable impact on the found particle size distribution due to the

different rates of particles sedimentation. The results well corresponding to the DLS analysis of the particle size distribution can be achieved if the sampling is performed immediately after shaking and from the middle part of the test tube.

The AFM measurements of Fe_2O_3 samples can also be influenced by the amount of the powder, which was dispersed. Too little an amount makes orientation on the sample difficult and hampers searching the particles (and their statistical analysis, as there are few particles in the scanning area), a large amount decreases the particle distinguishing, makes difficult setting up the feedback and leads to a greater particle agglomeration. In the case of the AFM analysis of Fe_2O_3, the optimal density of particles seems to be about 0.8 mg/ml H_2O.

In summary, the sample processing can influence the stability of the AFM measurement, the found particle size distribution, the general distribution of particles on the mica surface (and in the scanning area), the degree of particle agglomeration, and thus the image interpretation. Nevertheless, if the sample processing is optimized, high-quality images can be obtained as illustrated in the next chapters. The possibility to analyze the isolated particles without the presence of agglomerates (the nanoparticles deposited on the mica are well dispersed) is the main advantage of the described sample processing.
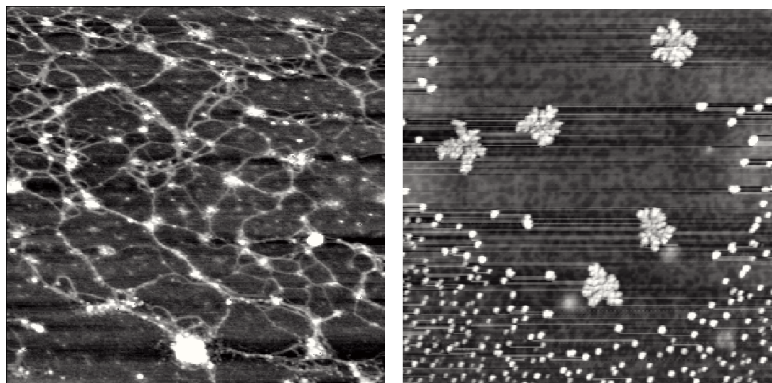

Figure 1: Effects related with the sample drying. A) Water chains among particles B) 2D clusters. (the scanning areas: 2×2 μm)

3   Image Processing, Artifacts and Measurement Interpretation.

To image the particles in a high quality, it is necessary to perform corrections of the sample slope and background. Regarding the instabilities created during scanning, especially in the ranges under 500×500 nm, it has been found useful to level the individual lines that will remove the image striping. The background spherical correction is another inevitable step to highlighting of the particles or their automatic analysis. Nevertheless, it is necessary to choose the sphere radius so that no deformation of the particle shape image occurs. If a particle size/scanning range ratio is lower than 1/10, this value can be used successfully as the sphere radius. It is not suitable to perform this processing when the particle takes a large part of the scanning area, because of a particle image deformation. It has been proved experimentally that the mentioned procedures do not greatly influence the given particle dimensions.

Several artifacts following from the scanning mechanism, the distance between probe and sample during the measurement, and quality of the sample affect imaging the Fe_2O_3 particles using the AFM method. As the typical artifact, the horizontal stripes (elevations) are created by catching a particle by the tip and its pulling to the edge of the scanning area. The main problem of AFM measurements is the space convolution of a sample with a tip, which distorts the particle shapes and increases their lateral dimensions. The shape distortion is obvious in line cross-sections, where the peak shape doesn't correspond to the particle profile but manifests the convolution effect. The profile of alpha Fe_2O_3 particles prepared by thermal treatment of $FeCO_3$ in air is shown on Fig. 2 to demonstrate the tip influence on the peak shapes. In the same figure, it is also possible to compare the profiles of isolated particles with the
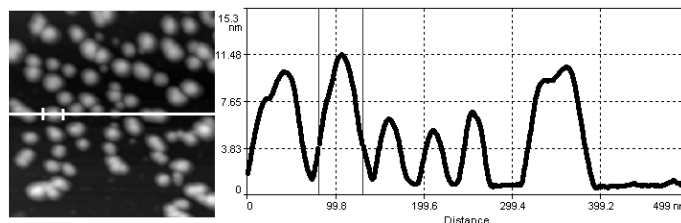
Figure 2: The line cross-section of α-Fe$_2$O$_3$ particles prepared by thermal treatment of FeCO$_3$

two-particle agglomerates (outer peaks with two maxima). Let us emphasize that some deconvolution process [11-13] should be applied to determine the actual particle size, especially in the case of analyzing ultrafine particles.

An extreme demonstration of convolution is the so called "tip imaging" which usually occurs during scanning the needle-like objects whose side slope is higher then the slope of the tip and the pyramidal or the conical shapes are observed. This artifact plays an important role also in the AFM analysis of Fe$_2$O$_3$ particles with the real size less than 10 nm, which appear as the small needles in 3D images. The AFM image of γ-Fe$_2$O$_3$ particles prepared by thermal decomposition of iron(II) oxalate shown on Fig. 3A illustrates suitably the effect of "tip imaging" on small particles.
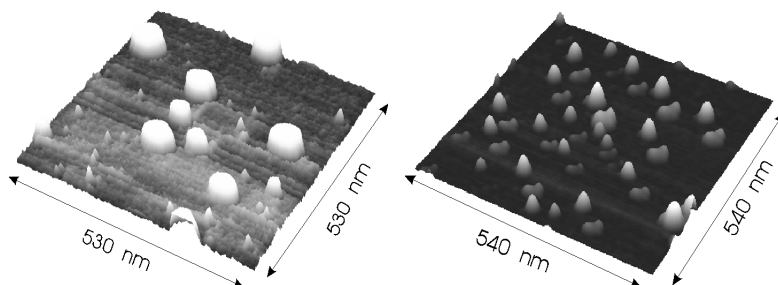

Figure 3: Convolution artifacts ("tip imaging" and "double-particles") in AFM images of γ-Fe$_2$O$_3$ nanopowders prepared by thermally induced oxidation of FeCO$_3$ (A) and FeSO$_4$ (B)

The other convolution artifacts can be related with the low tip quality. Doubled images oriented in the same manner clearly point at the double end of the tip. This artifact is most commonly manifested in measurements of iron oxide particles by the existence of "double-particles". The image of non-real particle is smaller and its orientation towards the real particle is maintained in the whole scanning area (Fig. 3B). The non-symmetric tip convolution may be manifested by elongation of the particles in one direction.

Several conclusions of the analyses of Fe$_2$O$_3$ nanoparticles follow from the convolution – it is impossible to determine correctly both the size and the morphology of very small particles (<10 nm), the morphology of nanoparticles can be assessed well in the size range of 10–100 nm (as demonstrated with the experimental examples – see the last chapters), the deconvolution process is necessary for the correct size characterization of particles.

Some artifacts are also related with setting the measurement parameters including the integral parameter of feedback, oscillation amplitude and the relative decrease of oscillation amplitude. As a result, these artifacts can lead both to the worsening of the visual quality and the image deformation. An important factor is the choice of the relative decrease of oscillation amplitude of cantilever. Its higher value (e.g. of 60 % compared to the standard 50 %) can lead to a better stability of measurement, however, the image resolution is then lower. On the other hand, lowering this parameter increases the probability of the undesirable interaction between the tip and the particles.

Regarding the construction of the Explorer microscope (a magnetic holder of both the sample and the cantilever) it is necessary to consider also the magnetism of the used particles as a very specific artifact. In AFM images of ferrimagnetic (gamma and epsilon) Fe$_2$O$_3$ particles, their magnetic orientation is

4

obvious, in comparison with paramagnetic β-Fe_2O_3 and/or antiferromagnetic α-Fe_2O_3. Nevertheless, the possibility of assessment of their morphology and size is maintained.

4 AFM in Studies of Iron(III) Oxides Formed During Thermal Processes

Solid-state thermal transformations of iron-bearing materials in an oxidizing atmosphere represent a simple and cheap way of synthesising Fe_2O_3 nanoparticles. The possibility to prepare a large amount of pure powder without any supporting material or matrix is a further advantage in comparison with other methods. Moreover, the properties of Fe_2O_3 nanoparticles can be successfully modified by the choice of the heating conditions and precursor properties (structure, morphology and crystallinity) [1]. In the next parts, the contribution of AFM microscopy in the study of Fe_2O_3 nanoparticles synthesized by thermal processes is demonstrated with three examples taken from our work in the field.

β-Fe_2O_3 and ε-Fe_2O_3 – the Rare Polymorphs with the Limited Size and Defined Morphology.
Beta and epsilon iron(III) oxides are less frequent polymorphs and only a few processes of their formation are mentioned [1-7,17-20]. β-Fe_2O_3 has a body-centered cubic "bixbyite" structure with $Ia\overline{3}$ space group, and two nonequivalent octahedral sites of Fe^{3+} ions in the crystal lattice. The cubic unit cell contains 32 Fe^{3+} ions, 24 of which have a C_2symmetry (d-position) and 8 a C_{3i} symmetry (b-position) [1-6]. ε-Fe_2O_3 is orthorhombic with space group $Pna2_1$. It is isomorphous with $AlFeO_3$, $GaFeO_3$, κ-Al_2O_3 and presumably ε-Ga_2O_3. In the structure there are three nonequivalent anion and four cation positions [7].

It is interesting, that all syntheses of β-Fe_2O_3 and ε-Fe_2O_3 powders are based on the thermal transformation of ferrogenous precursor. Due to the thermal instability of both polymorphs, hematite as product of their isochemical transformations appears in samples. Unfortunately, there are no literature data concerning the size of β-Fe_2O_3 particles synthesized by different thermal processes. On the other hand, the particle size of ε-Fe_2O_3, prepared by various methods, falls within the relatively narrow range of 30–80 nm [7,17]. So far a process of formation of large crystals of this polymorph has not been described.

To explain the mechanism of the thermally induced structural changes of β-Fe_2O_3 and ε-Fe_2O_3 to hematite and to assess the role of particle size in these transformations, we prepared both rare polymorphs by two different routes and analyzed them using AFM. The pure β-Fe_2O_3 powder was synthesized by the solid-state reaction of NaCl with $Fe_2(SO_4)_3$ [6], the sample with admixture of hematite was prepared by a thermal conversion of $Fe_2(SO_4)_3$ [5]. The AFM analysis revealed the presence of the relatively symmetric particles with the narrow size distribution (20–30 nm) in the pure β-Fe_2O_3 sample (Fig. 4A). The particles with the same size range and morphology were observed in the sample containing phase mixture. In addition, the larger hexagonal shape particles evidently corresponding to hematite, with the size above 100 nm were found in this sample. The absence of particles in the size range of 30–100 nm was registered as a surprising fact. Similarly, almost a pure ε-Fe_2O_3 sample was prepared by thermal transformation of γ-Fe_2O_3 nanoparticles formed from $FeSO_4$ [21], the sample with admixture of hematite was produced by a thermal conversion of $Fe_2(SO_4)_3$ under different experimental conditions than in the case of β-Fe_2O_3 formation [1]. In the pure ε-Fe_2O_3 sample, elongated particles with the narrow size range of 40–70 nm were detected (Fig. 4B). The size of ε-Fe_2O_3 is in agreement with observations of the authors, who synthesized this phase by other methods [7,17]. Particles of the same size and morphology were identified in the mixture sample, again, together with significantly larger (>150 nm) hexagonal particles of hematite.

Thus AFM measurements proved, that particles of both rare polymorphs are formed in a limited range during thermal processes. Further thermal sintering of particles, and therefore the increase of the particle size, probably induce the structural change into α-Fe_2O_3. Similar size-induced phase transitions have been observed during the thermal transformation of amorphous Fe_2O_3 particles (< 5 nm) to hematite via γ-Fe_2O_3 [22]. The origin of these structural transformations of nanocrystalline Fe_2O_3 particles can be found in the decrease of the unit-cell volume that occurs as the particle size is increased.
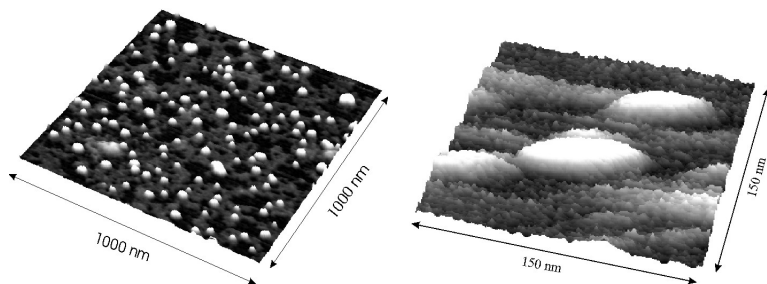
Figure 4: AFM images (cross-sections) of β-Fe$_2$O$_3$ nanoparticles prepared by solid-state reaction of NaCl with Fe$_2$(SO$_4$)$_3$ (A), and ε-Fe$_2$O$_3$ synthesized by thermal conversion of Fe$_2$(SO$_4$)$_3$ (B)

The Influence of Particle Morphology on the Color Quality of α-Fe$_2$O$_3$ Red Pigment Synthesized by Non-equivalent Routes. α-Fe$_2$O$_3$ (hematite) is the oldest-known and the most frequent inorganic pigment, chemically stable, non-toxic, non-bleeding and highly durable with excellent suspension properties and a very high heat resistance as a superior pigmentary characteristic. It is used in a wide range of applications, including paint and coatings, rubber and plastic products, textile finishes, building materials, and ceramics. Hematite has a rhombohedrally centered hexagonal structure of the corundum type (space group $R\bar{3}c$) with a close-packed oxygen lattice in which two thirds of the octahedral sites are occupied by Fe^{3+} ions. Its color quality is very sensitive particularly to the particle size, morphology and internal structure (cation substitution), and thus to the route of synthesis.

In the present example hematite powders were synthesized by "wet" route (by reacting a ferrous salt, a reducable aromatic nitrocompound and ammonium hydroxide, operating at a higher temperature, in an aqueous medium) and by the solid-state "dry" method (based on the thermal decomposition of FeSO$_4$·7H$_2$O in air). Both methods allow to control the particle size distribution by the choice of the experimental conditions, particularly using the change of the reaction temperature. Thus, hematite nanopowders with very uniform and almost the same particle size distributions were prepared. Mean particle diameters were determined from dynamic light scattering measurements: 90 and 92 nm for hematite prepared by wet and dry methods, respectively. Nevertheless, the measurements of the spectral reflectance curves revealed a significant difference in the color quality of both nanohematite samples.
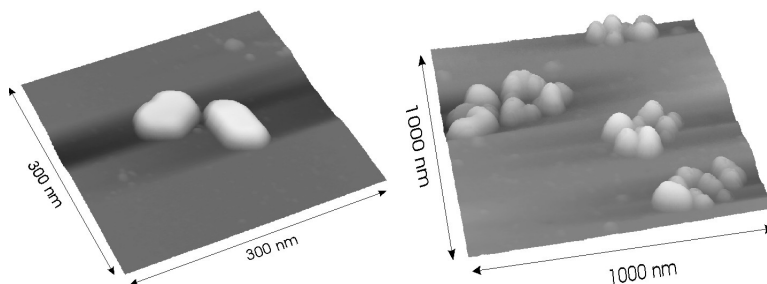

Figure 5: Hematite nanoparticles prepared by "wet" (A) and "dry" (B) ways

The AFM measurements were applied to asses the particle size and morphology and thus to explain the color difference. The hematite nanoparticles with the size of 85–90 nm (after deconvolution) and with the morphology corresponding to very thin hexagonal plates (the ratio of the major lateral dimension to vertical dimension: $d_l/d_v \sim 17$–25) were observed in AFM images of nanohematite prepared by wet route (see Fig. 5A as illustration). Particles of hematite prepared by solid-state method (Fig. 5B) show the size in the range of 80–100 nm and more symmetric rounded shapes ($d_l/d_v \sim 5$–10). Just the different values of vertical dimensions, which are responsible for different color quality, cannot be easily found by using other techniques including TEM.

Characterization of Amorphous Fe_2O_3 Prepared by Solid-State Reaction from Ammonium Ferrocyanide – AFM vs. TEM. Amorphous metal oxides have many important applications, including that in the fields of solar-energy transformation, magnetic storage media, electronics, and catalysis. An amorphous iron(III) oxide was prepared by various multistage "wet syntheses", where the initial iron containing precursor was in the form of solution ($Fe(CO)_5$ in decalin, iron(III) acetylacetonate in ethanol, $Fe(NO_3)_3$ in water, $FeCl_3$ in polyethylenglycol or butylacetate, iron perchlorate in acetonitrile) [22-27]. Authors agree that so-prepared oxide is composed from the nanometer-size particles (diameter is usually less than 7 nm). Van Diepen and Pompa [23] suggest that in amorphous Fe_2O_3, Fe^{3+} ions are surrounded by oxygen octahedra with the respective symmetry axes randomly orientated in non-periodic lattice.

The first pure solid-state synthesis based on the thermal decomposition of the solid ammonium ferrocyanide in air was realized in our laboratory. The chemical composition, magnetic properties, mechanism of thermal transformation, particle size and morphology of as-prepared Fe_2O_3 were investigated by different methods (XRD, SQUID magnetization measurements, Mössbauer spectroscopy, IR spectroscopy, measurement of thermomagnetic curves, TG/DTA, elemental and chemical analyses) including microscopic techniques. The prepared oxide was amorphous, well stoichiometric Fe_2O_3 showing the magnetic ordering temperature under 70 K, very narrow range of magnetic transition ($\sim$10 K) and the two-step thermal transformation to hematite (via maghemite). AFM and TEM analyses revealed, in the perfect correspondence, the particles multiple larger (60–120 nm) than those prepared by wet syntheses (Fig. 6). Concerning the particle morphology, AFM images show the vertically oblate ellipsoids ($d_l/d_v \sim 1/10$). This unique finding brings the completely new view on the amorphism of metal oxides and opens the door for their new applications.
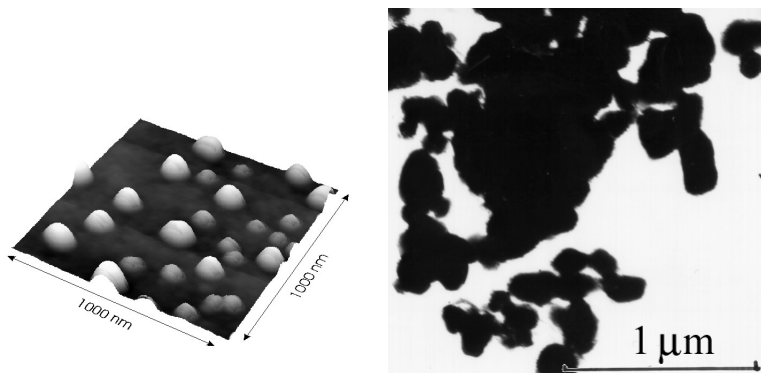

Figure 6: AFM (A) and TEM (B) images of amorphous Fe_2O_3 particles prepared by thermal decomposition of ammonium ferrocyanide in air.

Summary

AFM is a powerful technique for the characterization of nanopowders, although its use for the characterization of particles smaller than 10 nm is restricted due to the strong influence of the tip convolution. In the range of 10–100 nm, AFM brings information about the particle size, comparable with the TEM technique. The possibility to determine the vertical dimension allows to achieve the superior (in comparison with TEM) morphological characterization. The example of iron(III) oxides indicates that AFM is very effective in the analysis of the powdered polymorphous mixtures since the ratio of lateral to vertical dimensions can be used as the tool for distinguishing the structurally non-equivalent particles. Thus the particle size of individual polymorphs contained in the phase mixture can be evaluated.

References

[1] R. Zboril, M. Mashlan and D. Petridis: Chemistry of Materials Vol. 14 (2002), p. 969.

[2] R. M. Cornel and U. Schwertmann: The Iron Oxides. Structure, Properties, Reactions and Uses, (VCH, Weinheim 1996).

[3] T. Muruyama and T. Kanagawa: J. Electrochem. Soc.Vol. 143 (1996), p. 1675.

[4] T. Gonzales-Carreno, M.P. Morales and C.J. Serna: J. Mater. Sci. Lett. Vol. 13 (1994), p. 381.

[5] R. Zboril, M. Mashlan, D. Krausova and P. Pikal: Hyperfine Interact. Vol. 121-122 (1999), p. 497.

[6] R. Zboril, M. Mashlan and D. Krausova: in Mössbauer Spectroscopy in Materials Science (Eds.: M. Miglierini, D. Petridis), (Kluwer Academic Publishers, Dordrecht 1999), p. 49.

[7] E. Tronc, C. Chanéac and J. P. Jolivet: J. Solid State Chem. Vol. 139 (1998), p. 93.

[8] T. Hyeon, S.S. Lee, J. Park, Y. Chung and H.B. Na: J. Am. Chem. Soc. Vol. 123 (2001), p. 12798.

[9] Z.Y. Zhong, T. Prozorov, I. Felner and A. Gedanken: J. Phys. Chem. B Vol. 103 (1999), p. 947.

[10] R.D. Zysler, M. Vasquez-Mansilla, C. Arciprete, M. Dimitrijewits, D. Rodriguez-Sierra and C. Saragovi: J. Magn. Magn. Mater. Vol. 224 (2001), p. 39.

[11] D.L. Wilson, K.S. Kump, S.J. Eppell and R.E. Marchant: Langmuir Vol. 11 (1995), p. 265.

[12] D.Q. Yang, Y.Q. Xiong, Y. Guo, D.A. Da and W.G. Lu: J. Mater. Sci. Vol. 36 (2001), p. 263.

[13] D.J. Keller and F.S. Franke: Surf. Sci. Vol. 294 (1993), p. 409.

[14] C. Liu and P. M. Huang: Soil. Sci. Soc. Am. J. Vol. 63 (1999), p. 65.

[15] X. Zeng, N. Koshizaki and T. Sasaki: Appl. Phys. A Vol. 69 (1999), p. S253.

[16] L.M. Lacava, B.M. Lacava, R.B. Azevedo, Z.G.M. Lacava, N. Buske, A.L. Tronconi and P.C. Morais: J. Magn. Magn. Mater. Vol. 225 (2001), p. 79.

[17] R. Schrader and G. Büttner: Z. Anorg. Allg. Chem. Vol. 320 (1963), p. 220.

[18] J. L. Dormann, N. Viart, J. L. Rehspringer, A. Ezzir and D. Niznansky: Hyperfine Interact. Vol. 112 (1998), p. 89.

[19] I. Dézsi and J. M. D. Coey, Phys. Status. Solidi A Vol. 15 (1973), p. 681.

[20] K. Barcova, M. Mashlan, R. Zboril, P. Martinec and P. Kula: Czech. J. Phys. Vol. 51 (2001), p. 749.

[21] R. Zboril, M. Mashlan and D. Krausova: Czech. J. Phys. Vol. 51 (2001), p. 719.

[22] P. Ayyub, M. Multani, M. Barma, V.R. Palkar and R. Vijayaraghavan, J. Phys. C: Solid State Phys. Vol. 21 (1988), p. 2229.

[23] A. M. van Diepen and T. J. A. Popma, J. Phys. Colloque (Paris) C6 Vol. 37 (1976), p. 755.

[24] X. H. Liao, J. J. Zhu, W. Zhong and H.Y. Chen: Mater. Lett. Vol. 50 (2001), p. 341.

[25] G. Zotti, G. Schiavon, S. Zecchin and U. Casellato: J. Electrochem. Soc. Vol. 145 (1998), p. 385.

[26] K. Prabhakaran, K.V.P.M. Shafi, A. Ulman and T. Ogino: Adv. Mater. Vol.13 (2001), p. 1859.

[27] K. Tanaka, K. Kamiya, M. Matsuoka, T. Yoko: J. Non-Cryst. Solids Vol. 94 (1987), p. 365.